Paper:
Zhu, P., Zhao, Z., Nie, J., Hu, G., Li, L. & Zhang, Y. (2018). Ultra-high sensitivity strain sensor based on piezotronic bipolar transistor. *Nano Energy, 50*, 744-749.
http://dx.doi.org/10.1016/j.nanoen.2018.06.035

Ultra-High Sensitivity Strain Sensor based on Piezotronic Bipolar Transistor

Ziming Zhao [1,†], Ping Zhu [1,†], Jiaheng Nie [1], Gongwei Hu [1], Lijie Li [2,*], and Yan Zhang [1,3,4,*]

[1] *School of Physics, School of Physical Electronics, University of Electronic Science and Technology of China, Chengdu 610054, China*

[2] *Multidisciplinary Nanotechnology Centre, College of Engineering, Swansea University, Swansea, SA1 8EN, UK*

[3] *Beijing Institute of Nanoenergy and Nanosystems, Chinese Academy of Sciences, Beijing 100083, China*

[4] *College of Nanoscience and Technology, University of Chinese Academy of Sciences, Beijing 100049, China*

[†] These authors contributed equally to this work.

[*] To whom correspondence should be addressed, E-mail: zhangyan@uestc.edu.cn and L.Li@swansea.ac.uk

Abstract

Due to the coupling of piezoelectric and semiconductor properties, the wurtzite structure semiconductors have been used for fabricating high performance piezotronic devices. The carrier transport behavior can be effectively controlled by the polarized charges induced by applied strain. High-sensitive piezotronic strain sensors have potential application in next generation self-powered, flexible electronics and wearable systems. In this study, a piezotronic bipolar transistor has been studied through theoretical calculation and numerical simulation. The output current, gauge factor and carrier concentration have been simulated under the influence of different strains. The piezotronic bipolar transistor based strain sensor has ultrahigh sensitivity and the gauge factor can reach over 10^4. This investigation not only provides a theoretical insight into the piezotronic effect on bipolar transistor, but also presents a new approach to design ultra-high sensitivity strain sensor.

Keywords: piezotronics, bipolar transistor, ultrahigh sensitivity strain sensor

1. Introduction

Piezoelectric semiconductors, such as ZnO, GaN, InN, CdS and monolayer MoS2, have recently attracted widespread attention for innovative pieozotronic and piezophototronic devices [1] ; [2], such as nanogenerators [3]; [4] ; [5], piezoelectric field-effect transistors [6], high sensitivity piezotronic strain sensor [7], taxel-addressable matrices [8], photon-strain sensor arrays [9], single-atomic-layer MoS2 piezotronic transistor [10], and strain control piezotronic logic devices [11]. Piezotronic nanodevices show potential application because of its high performance by using strain-induced piezoelectric charges to modulate the transport characteristics. [12] High-resolution dynamic pressure sensor array based on a composite of sandwiching InGaN/GaN multiple quantum wells (MQW) between p-AlGaN/p-GaN layers and n-GaN layers display a high photoluminescence intensity by small strain range (0–0.15%) [13]. A flexible GaN membrane-based ultraviolet photoswitch exhibits on-to-off ratio of up to 4.67×10^5[14]. A two-terminal piezotronic transistor using ZnO twin nanoplatelet by the mirror symmetrical structure has a high sensitivity property of 1448.08 − 1677.53 meV/MPa [15]. Electric skins have been demonstrated based on the low-power or self-powered properties [16]. Moreover, piezotronic strain sensor can be used for designing piezotronic analog-to-digital converter devices for strain imaging and analog computing [17]. Piezotronic integrated chips have been developed next generation self-powered, flexible electronics and wearable systems [12].

High sensitivity, fast response, and low power consumption are key characteristics of sensors for internet of things and self-powered applications. Using strains to effectively control carrier transport in nanodevices is one of important ways to design high sensitivity strain sensors. Because the strain-induced piezoelectric field can precisely control carrier transport, the first reported piezotronic strain sensor demonstrated an ultra-high gauge factor (GF) ~1250 [7]. In comparison with the carbon-based high sensitivity devices, the strain sensor can also be developed based on carbon nanotubes (CNTs) with GF ~1000 [18]. A strain sensor based on the composite of reduced graphene oxide microtubes‒elastomer with polymer coating process has the GF of 630 with the strain range of 21.3% [19]. By using high conductivity performance of the carbon/graphene composites nanofiber yarn (CNY), GF value of the strain sensor can achieve 416 [20]. An electromechanical sensor has been reported to detect small stresses with GF above 500, by assembling graphene and lightly crosslinked polysilicone. [21] For silicon-based devices, flexible strain sensors fabricated fabric consisting of long Si nanowires demonstrate gauge factor of up to 350, which can be employed to detect human motions or broader applications in other wearable devices [22]. Polymer materials show highly stretchable, for example, a sensor with two interlocked arrays of high-aspect-ratio Pt-coated polymeric nanofibers on the surface of thin polydimethylsiloxane layers exhibits strain detection sensitivity of about 11.45 GF [23].

Although the on-off process is another way to design high sensitivity strain sensors, the design is more suitable for strain trigger or switch applications. For example, mechanical crack-based sensor shows a gauge factor of above 2000, based on disconnection–reconnection with nanoscale crack junctions. [24] However, the strain only varies from 0% to 2%. Recent theoretical results found ultra-high on-off ratio up to 10101010 for an excellent strain-controlled switch by using piezoelectric potential to control the quantum states of HgTe quantum well topological insulator [25], indicating piezotronic devices will show higher gauge factor and larger strain range in on-off mode devices.

In this study, we theoretically demonstrate piezotronic bipolar transistor for designing ultra-high sensitivity sensor. The mechanism of piezotronic strain sensor is that piezopotential by strain-induced piezoelectric charges can change the built-in electric potential in junction or local Schottky barrier height in metal-semiconductor contact, and control the carrier transport. Bipolar transistor is a three-terminal device including base, emitter, and collector, as shown in Fig. 1(a). In this work, we investigate current-voltage characteristics of piezotronic bipolar transistors in the common-emitter model under the influence of externally applied strains. The base and emitter have different piezoelectric property. While a strain is supplied to the transistor, piezoelectric charges will be induced at the interface of base-emitter junction, as shown in Fig. 1(b) and (c). Therefore, carriers transport in the bipolar transistor can be effectively controlled by the strain. A piezoelectric bipolar transistor model has been established using a p-n-p or n-p-n structure. Finite element method (FEM) simulation presents the variation of the carrier transport at the emitter-base junction under applied strain. The basic principle provides not only a deeper understanding for the mechanism of ultrahigh sensitivity piezotronic strain sensors, but also an innovative and practical approach for designing ultrahigh sensitivity strain sensors.

2. Ultra-high sensitivity strain sensor based on piezotronic bipolar transistor

The p-n junctions play key role in electronic devices. In a bipolar transistor, there are two p-n junctions in series connection, which leads to two doping types in the devices: n-p-n type and p-n-p type. The piezoelectric material is located at the intermediate layer. Taking n-p-n type piezotronic bipolar transistor as an example, p-type and n-type are chosen as semiconductor material with different piezoelectric property. Base and emitter are made by different piezoelectric coefficient materials. Typical design also includes p-n junction of nonpiezoeletric and piezoelectric material, and opposite growth direction of same piezoelectric semiconductor. The strain-induced piezoelectric charges are distributed within the width of W_{piezo} at the interface of left p-n junction, as shown in Fig. 2(a). The band structure and carrier transport characteristics of the transistor will be changed by applied strain. Depending on which lead is common to the input and output circuits, bipolar transistor can be connected in three circuit configurations: the common-base, common-emitter, and common-collector configurations. For n-p-n transistor connected in common-emitter configurations as example, base-emitter voltage V_{BE} is forward biased and collector-emitter voltage V_{CE} is reverse biased. Thus, the V_{BE} is external bias voltage in our BJT model, so the external strain modulate the build-in potential of emitter-base junction, and does not change the voltage V_{BE}. For simplicity, the DC parameters are assumed as constants in this manuscript. The DC parameters, for example, current gain beta factor generally varies with collector current. Thus, the DC parameters of BJT can be modulated by strain-induced piezoelectric field.

When bipolar transistor is biased in normal mode [26], the electronic current at the emitter terminal I_{nE} and the collector terminal I_{nC} are given by

$$\begin{cases} I_{nC} = \dfrac{A_E q D_n n_{p0}}{L_n} \cos ech\left(\dfrac{W}{L_n}\right) \exp\left(\dfrac{qV_{BE}}{kT}\right) \\ I_{nE} = \dfrac{A_E q D_n n_{p0}}{L_n} \coth\left(\dfrac{W}{L_n}\right) \exp\left(\dfrac{qV_{BE}}{kT}\right) \end{cases} \tag{1}$$

where A_E is the cross-sectional area of the emitter-base junction, q is the absolute value of the unit electronic charge, W is the width of base region, n_{p0} is the thermal equilibrium electron concentration in the p-type semiconductor, $L_n = \sqrt{D_n \tau_n}$ are diffusion lengths of holes, D_n is the diffusion coefficients for electrons.

For the common-emitter mode, the terminal current should meet the following relation in the absence of strain

$$I_{B0} = I_{E0} - I_{C0} \tag{2}$$

where I_{B0}, I_{E0} and I_{C0} are the initial base current, emitter current and collector current, respectively.

While a mechanical strain is supplied to the bipolar transistor, the base current will be changed by a α factor that is associated with the piezoelectric charges [27].

$$I_B = \alpha I_{B0} = \exp\left(\frac{q^2 \rho_{piezo} W_{piezo}^2}{2\varepsilon_s kT}\right) I_{B0} \tag{3}$$

where ρ_{piezo} is the density of piezoelectric charges.

The collector current can be obtained from the base current times a β factor

$$I_C = \beta I_B = \beta \exp\left(\frac{q^2 \rho_{piezo} W_{piezo}^2}{2\varepsilon_s kT}\right) I_{B0} \tag{4}$$

For wurtzite structure GaN, the density of piezoelectric charges can be obtained from equation (5) while the strain is applied only along the c-axis direction

$$P = q\rho_{piezo} W_{piezo} = e_{33} s_{33} \tag{5}$$

where e_{33} is the piezoelectric coefficient and s_{33} is the applied strain.

The current sensitivity of piezoelectric bipolar transistor can be defined as

$$R = \frac{dI_C}{ds_{33}} = \frac{qe_{33}W_{piezo}}{2\varepsilon_s kT} I_C \tag{6}$$

where R is the sensitivity of output current by applying a strain.

Gauge factor determining the performance of transistor is given by

$$G = \frac{d\left[I_C(s_{33})/I_C(0)\right]}{ds_{33}} = \frac{\beta qe_{33}W_{piezo}}{2\varepsilon_s kT} \exp\left(\frac{qe_{33}s_{33}W_{piezo}}{2\varepsilon_s kT}\right) \tag{7}$$

The I-V characteristic of base current is illustrated in Fig. 2(b) with the strain range from -1.0% to 1.0%. Fig. 2(c) shows the base current I_B and collector current I_C as a function of strain while the stain varies from -10% to 4%. The currents increase exponentially with the strain. The gauge factor can be used to describe the high-performance feature of the piezotronic bipolar transistor and is shown in Fig. 2(d). The gauge factor also presents the exponential increase with strain and typically can reach over 10^4. This value is at less several orders of magnitude higher than previously reported strain sensors. The sensitivity of a strain sensor is dimensionless quantity, depicted by a GF.

Using piezotronic effect, the base current IBIB across emitter-base junction can be modulated by external applied strain. For common-emitter circuit configuration, piezotronic bipolar transistor can amplify current. Due to large current gain I_C/I_B, the collector current I_C has very large change with various strain. This is the mechanism of ultrahigh sensitivity of piezotronic BJT. Therefore, piezotronics have not only great impact on the flexible electronics, but also semiconductor physics field. Piezotronic BJTs also offer new semiconductor technology, such as piezoelectric semiconductor crystal growth, device design and fabrication, and integration.

3. Numerical Simulation of Piezotronic Bipolar Transistor

The analytical solution of the bipolar transistor gives only qualitative insight into the modulation mechanism of strain-induced piezoelectric charges at the p-n junction interface. Numerical simulation of the piezotronics bipolar transistor can give more precise quantitative results. Our earlier work [28] provided a single junction model to explain the piezotronic and piezophototronic effect on diode and LED, which are two-terminal devices. The present modeling framework provides a three-terminal device which includes two junctions. Strain-induced piezoelectric field can be used to control the carrier transport, generation and combination in junction region, which is principle of piezotronic and piezo-phototronics effect.

In order to describe the piezotronic effect on the bipolar transistor, the fundamental governing equations including electrostatic equations, current density equations and continuity equations should be given. The electrical property of the piezotronic bipolar transistor can be obtained from the basic equations under the special boundary conditions. In the numerical simulation of a bipolar transistor, ideal Ohmic contacts are considered at the base, collector and emitter. This indicates that the carrier concentration and electrical potential should satisfy the Dirichlet boundary condition while they are applied at the transistor boundaries. The strain-induced piezoelectric charges are distributed at the interface between base and emitter.

In this study, we employ the COMSOL software package for numerically solving the basic equations of the n-p-n type bipolar transistor. The DC characteristics of the bipolar transistor are mainly investigated under an uniform strain. The piezoelectric charges obtained from Eq. (5) are distributed at the interface between p+ side and n side within the width WpiezoWpiezo. The p-type doping layer is set as piezoelectric semiconductor GaN and two n-type doping layers are chosen as silicon.

The schematic of the n-p-n type piezotronic bipolar transistor is shown in Fig. 3(a). Fig. 3(b) plots the net doping concentration as a function of the depth without strain. Three distinct regions can be clearly shown and respectively correspond to different doping types. Piezotronics is novel field based on piezoelectric semiconductor, which have great potential in next generation sensor and energy application. According to Shockley theory, our previous theoretical works have studied piezotronic-modulated depletion [29]. Although carrier concentration in base layers is 10 times larger than the collector doping, the piezoelectric charges can effectively control carrier transport properties in depletion region of BJT. Fig. 3(c) calculates three terminal currents varying with the base-emitter voltage V_{BE} while the strain is absent and the collector-emitter voltage V_{CE} is fixed at 2 V. The current increases with the voltage. Fig. 3(d) shows the base current and the collector current as a function of the base-emitter voltage at different strains. For a fixed voltage V_{BE}, the current increases with strain.

We also simulate this type of bipolar transistors and compute the electrical characteristics under different strains. Fig. 4(a) presents the collector current as a function of the collector voltage under the strain varying from − 1 to 1% when the collector-emitter voltage is fixed at 2 V. With the voltage increasing from 0 V to 3.0 V, the current increases sharply at the beginning and slowly for the voltage larger than 0.2 V. Obviously, the current also increases with the increase of the strain. Our analytical results provide a method for calculating gauge factor of sensor based on piezotronic bipolar transistors. The analytical results are normal mode which has no clear saturation in the collector current. For our results by finite element calculation, the simulation results show four mode of BJT, thus, Fig. 4(a) shows saturation region. The gauge factor value calculated by COMSOL to simulate the sensitivity of a strain sensor device is demonstrated in Fig. 4(b). The dynamic characteristics are very important for piezotronic BJT, which include high-frequency, high-power, and switching behaviors. Transit time and charge storage can be modulated by strain-induced piezoelectric charges in depletion region. Figs. 4(c) and (d) show the electron and hole concentrations along the device. The peak position is at the piezoelectric charge distribution region. When the strain is varied from 0% to 1%, the electron concentration increases, and the concentration of the hole has a very little change. The simulation provides the distributions with various strains, which depend on doping profile, carrier transport, generation, and recombination. The numerical results show that the piezotronic effect provides small changes of the carrier distributions. Because the basic function of amplify current, piezotronic bipolar transistor can obtain good performance for strain sensor application. When piezoelectric charges created by external applied strain in piezotronic BJT, the electron and hole currents are modulated by piezoelectric charges. Small change of base current can induce large change. Strain-induced piezoelectric charges enhance the collector current. Thus, the ultrahigh strain sensitivity can be obtained. Recent experimental results reports that two back-to-back bulk ZnO with reversely growing directions can realize a great gauge factor approaching to 800 [30]. The experimental approaches provide a good solution for fabricating the piezotronic bipolar transistors.

4. Summary

In summary, we demonstrate the basic principle of the piezoelectric bipolar transistor by introducing the process of the charge transport across the emitter-base junction with the generation of piezopotential upon an applied strain. Piezoelectric semiconductors of wurtzite materials such as ZnO, GaN, coupling piezotronics and semiconductor properties, offer significant current gains even though under a very small mechanical strain, which is far higher than traditional CNT or graphene transistor. Thus, piezotronic bipolar transistors based on GaN can achieve ultrahigh sensitivity with the gauge factor of 10^4 upon only 2% strain, which is the highest to the best of our knowledge. Systemic theoretical investigation of the piezoelectric bipolar transistor in this study can have a paradigm shift in the way of designing the next generation NEMS and human-electronic sensor-based systems.

Acknowledgements

The authors are thankful for the support from University of Electronic Science and Technology of China (ZYGX2015KYQD063) , Swansea University, SPARC II project, and Thousand Talents program for a pioneer researcher and his innovation team, China.

References

[1] W. Wu, Z.L. Wang, Nat. Rev. Mater. 1 (2016).
[2] Z.L. Wang, Nano Today 5 (2010) 540–552.
[3] Z.L. Wang, J.H. Song, Science 312 (2006) 242–246.
[4] X. Wang, J. Song, J. Liu, Z.L. Wang, Science 316 (2007) 102–105.
[5] Y. Qin, X. Wang, Z.L. Wang, Nature 451 (2008) 809–813.
[6] X. Wang, J. Zhou, J. Song, J. Liu, N. Xu, Z.L. Wang, Nano Lett. 6 (2006) 2768–2772.
[7] J. Zhou, Y. Gu, P. Fei, W. Mai, Y. Gao, R. Yang, G. Bao, Z.L. Wang, Nano Lett. 8(2008) 3035–3040.
[8] W. Wu, X. Wen, Z.L. Wang, Science 340 (2013) 952–957.
[9] C. Pan, L. Dong, G. Zhu, S. Niu, R. Yu, Q. Yang, Y. Liu, Z.L. Wang, Nat. Photonics 7(2013) 752–758.
[10] W. Wu, L. Wang, Y. Li, F. Zhang, L. Lin, S. Niu, D. Chenet, X. Zhang, Y. Hao, T.F. Heinz, J. Hone, Z.L. Wang, Nature 514 (2014) 470–474.
[11] W. Wu, Y. Wei, Z.L. Wang, Adv. Mater. 22 (2010) 4711–4715.
[12] W. Wu, C. Pan, Y. Zhang, X. Wen, Z.L. Wang, Nano Today 8 (2013) 619–642.
[13] M. Peng, Z. Li, C. Liu, Q. Zheng, X. Shi, M. Song, Y. Zhang, S. Du, J. Zhai, Z.L. Wang, ACS Nano 9 (2015) 3143–3150.
[14] M. Peng, Y. Liu, A. Yu, Y. Zhang, C. Liu, J. Liu, W. Wu, K. Zhang, X. Shi, J. Kou, J. Zhai, Z.L. Wang, ACS Nano 10 (2016) 1572–1579.
[15] L. Wang, S. Liu, X. Feng, Q. Xu, S. Bai, L. Zhu, L. Chen, Y. Qin, Z.L. Wang, ACS Nano 11 (2017) 4859–4865.
[16] R. Yu, L. Dong, C. Pan, S. Niu, H. Liu, W. Liu, S. Chua, D. Chi, Z.L. Wang, Adv. Mater. 24 (2012) 3532–3537.
[17] J. Nie, G. Hu, L. Li, Y. Zhang, Nano Energy 46 (2018) 423–427.
[18] J. Cao, Q. Wang, H. Dai, Phys. Rev. Lett. 90 (2003) 157601.
[19] Y. Tang, Z. Zhao, H. Hu, Y. Liu, X. Wang, S. Zhou, J. Qiu, ACS Appl. Mater. Interfaces 7 (2015) 27432-27439.
[20] T. Yan, Z. Wang, Y.-Q. Wang, Z.-J. Pan, Mater. Des. 143 (2018) 214–223.
[21] C.S. Boland, U. Khan, G. Ryan, S. Barwich, R. Charifou, A. Harvey, C. Backes, Z. Li, M.S. Ferreira, M.E. Mobius, R.J. Young, J.N. Coleman, Science 354 (2016)1257–1260.
[22] B.C. Zhang, H. Wang, Y. Zhao, F. Li, X.M. Ou, B.Q. Sun, X.H. Zhang, Nanoscale 8 (2016) 2123–2128.
[23] C. Pang, G.Y. Lee, T.I. Kim, S.M. Kim, H.N. Kim, S.H. Ahn, K.Y. Suh, Nat. Mater. 11 (2012) 795–801.
[24] D. Kang, P.V. Pikhitsa, Y.W. Choi, C. Lee, S.S. Shin, L. Piao, B. Park, K.Y. Suh, T.I. Kim, M. Choi, Nature 516 (2014) 222–226.
[25] G. Hu, Y. Zhang, L. Li, Z.L. Wang, ACS Nano 12 (2018) 779–785.
[26] S.M. Sze, K.K. Ng, Physics of Semiconductor Devices, 3rd edition, John wiley & sons, New Jersey, 2007.
[27] Y. Zhang, Y. Liu, Z.L. Wang, Adv. Mater. 23 (2011) 3004–3013.
[28] Y. Zhang, Z.L. Wang, Adv. Mater. 24 (2012) 4712–4718.
[29] Y. Liu, Y. Zhang, Q. Yang, S. Niu, Z.L. Wang, Nano Energy 14 (2015) 257–275.
[30] R. Baraki, N. Novak, T. Frömling, T. Granzow, J. Rödel, Appl. Phys. Lett. 105 (2014) 111604.

Figure caption

Fig. 1. Schematic of the n-p-n type and p-n-p type piezotronic bipolar transistor. (a) A typical three-terminal diagram without strain and (b) with strain. The intermediate layer is piezoelectric semiconductor material and the induced piezopotential has opposite signs for tensile and compressive strain.

Fig. 2. The p-n-p type piezotronic bipolar transistor in the presence of strain. (a) The distribution of the piezoelectric charges, acceptors concentration and donors concentration and the corresponding energy band diagram (dotted line for with strain and solid line for without strain). (b) The base current and collector current varying with the voltage under different strains. (c) The base current and the collector current versus strain. (d) The gauge factor as a function of strain.

Fig. 3. The numerical simulation of the p-n-p type piezotronic bipolar transistor. (a) Schematic of a piezotronic GaN nanowire bipolar transistor. (b) The distribution of the net doping concentration as a function of the depth. (c) Currents of three terminals versus the base-emitter voltage. (d) The base current and (d) collector current varying with the strain.

Fig. 4. The numerical simulation of the n-p-n type piezotronic bipolar transistor under different strains. (a) The collector current as a function of collector voltage. (b) The gauge factor as a function of strain. The distribution of (c) electron concentration and (d) hole concentration for fixed collector-emitter voltage (VCE = 2 V).

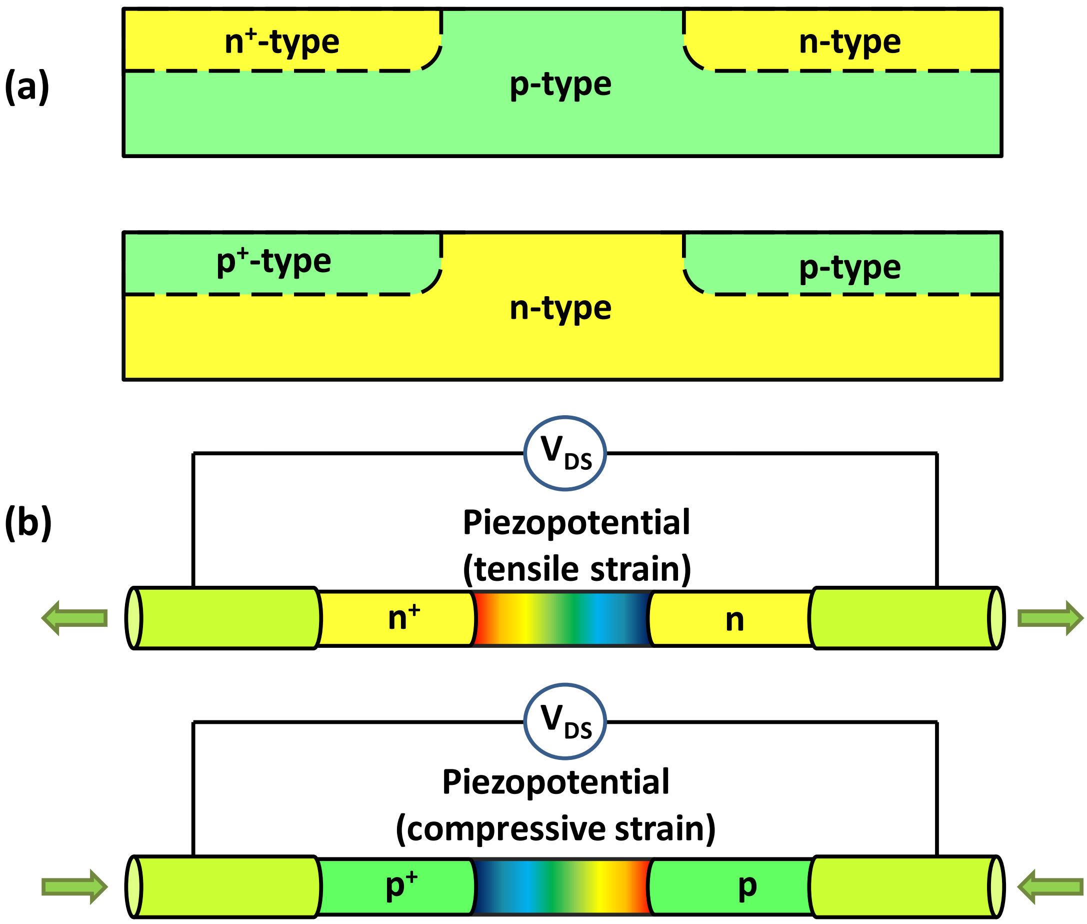

(a)
n+-type
n-type
p-type
p+-type
p-type
n-type
(b)
VDS
Piezopotential
(tensile strain)
n+
n
VDS
Piezopotential
(compressive strain)
p+
p

Fig. 1

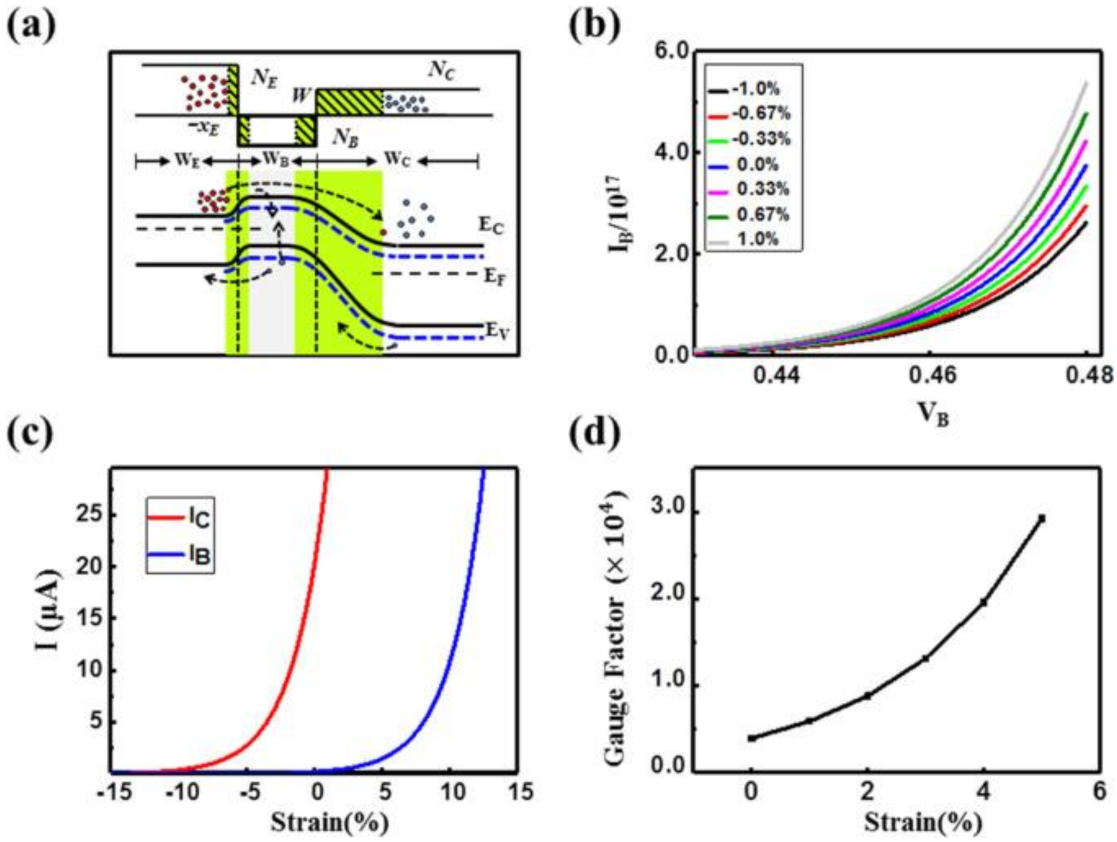
(a)
N_E
N_C
W
$-x_E$
N_B
W_E
W_B
W_C
E_C
E_F
E_V
(b)
-1.0%
-0.67%
-0.33%
0.0%
0.33%
0.67%
1.0%
$I_B/10^{17}$
V_B
(c)
I_C
I_B
I (μA)
Strain(%)
(d)
Gauge Factor (× 10^4)
Strain(%)

Fig. 2

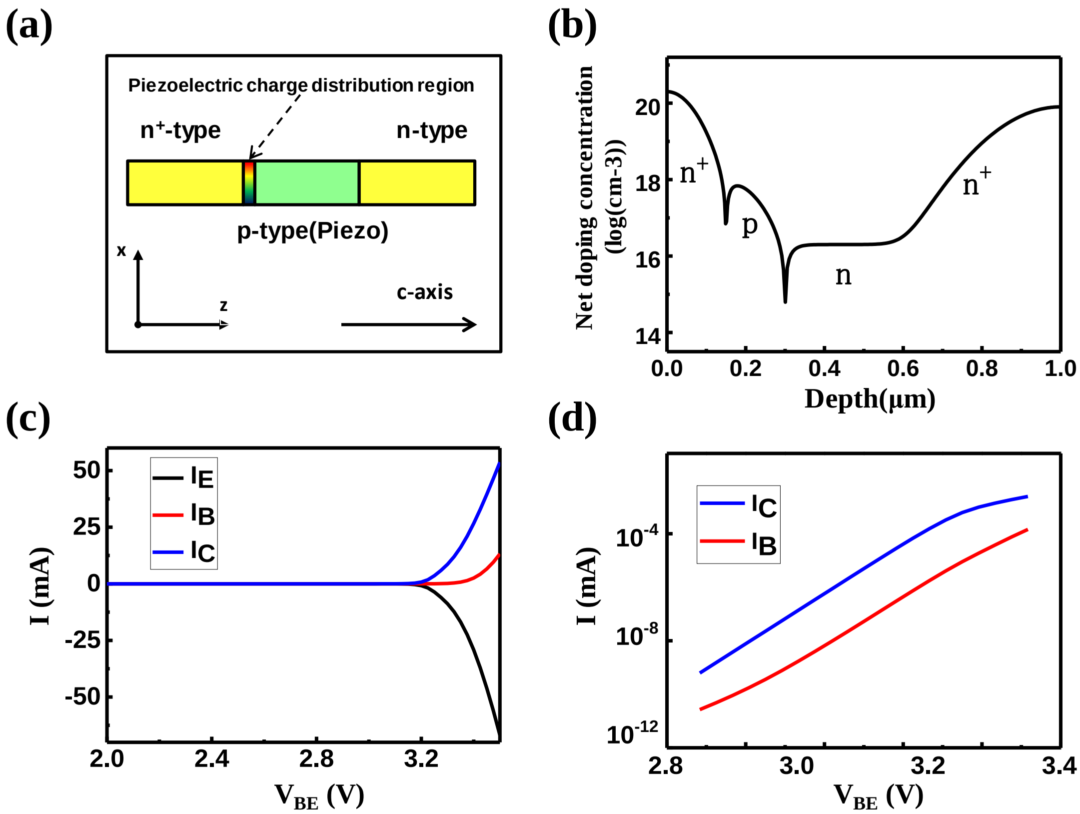

(a)
Piezoelectric charge distribution region
n+-type
n-type
p-type(Piezo)
x
z
c-axis
(b)
Net doping concentration (log(cm-3))
n+
p
n
n+
Depth(μm)
(c)
I (mA)
IE
IB
IC
VBE (V)
(d)
I (mA)
IC
IB
VBE (V)

Fig. 3

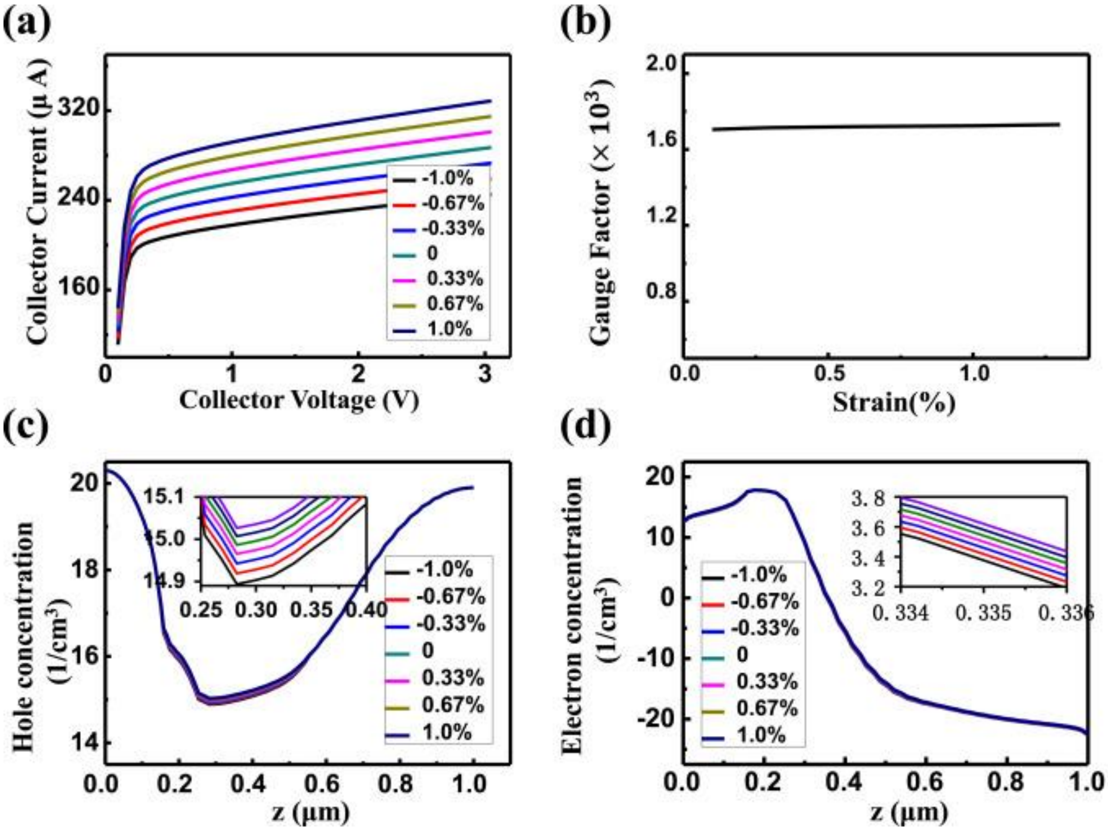

(a)
Collector Current (μ A)
320
240
160
0
1
2
3
Collector Voltage (V)
-1.0%
-0.67%
-0.33%
0
0.33%
0.67%
1.0%
(b)
Gauge Factor (× 10^3)
2.0
1.6
1.2
0.8
0.0
0.5
1.0
Strain(%)
(c)
Hole concentration (1/cm^3)
20
18
16
14
0.0
0.2
0.4
0.6
0.8
1.0
z (μm)
15.1
15.0
14.9
0.25
0.30
0.35
0.40
-1.0%
-0.67%
-0.33%
0
0.33%
0.67%
1.0%
(d)
Electron concentration (1/cm^3)
20
10
0
-10
-20
0.0
0.2
0.4
0.6
0.8
1.0
z (μm)
3.8
3.6
3.4
3.2
0.334
0.335
0.336
-1.0%
-0.67%
-0.33%
0
0.33%
0.67%
1.0%

Fig. 4